

Quantitative analysis of epithelial morphogenesis in *Drosophila* oogenesis: New insights based on morphometric analysis and mechanical modeling

K.S. Kolahi ^{a,1}, P.F. White ^{a,1}, D.M. Shreter ^{a,1}, A.-K. Classen ^{b,1}, D. Bilder ^{b,*}, M.R.K. Mofrad ^{a,*}

^a Molecular Cell Biomechanics Laboratory, Department of Bioengineering, University of California, Berkeley, 208A Stanley Hall #1762, Berkeley, CA 94720-1762, USA

^b Department of Molecular and Cellular Biology, University of California, 142 LSA #3200, Berkeley, CA 94720-3200, USA

ARTICLE INFO

Article history:

Received for publication 21 November 2008

Revised 16 April 2009

Accepted 23 April 2009

Available online 3 May 2009

Keywords:

Epithelial morphogenesis
Drosophila melanogaster oogenesis
 Mechanics
 Morphometric analysis
 Computational modeling

ABSTRACT

The process of epithelial morphogenesis is ubiquitous in animal development, but much remains to be learned about the mechanisms that shape epithelial tissues. The follicle cell (FC) epithelium encapsulating the growing germline of *Drosophila* is an excellent system to study fundamental elements of epithelial development. During stages 8 to 10 of oogenesis, the FC epithelium transitions between simple geometries—cuboidal, columnar and squamous—and redistributes cell populations in processes described as posterior migration, squamous cell flattening and main body cell columnarization. Here we have carried out a quantitative morphometric analysis of these poorly understood events in order to establish the parameters of and delimit the potential processes that regulate the transitions. Our results compel a striking revision of accepted views of these phenomena, by showing that posterior migration does not involve FC movements, that there is no role for columnar cell apical constriction in FC morphogenesis, and that squamous cell flattening may be a compliant response to germline growth. We utilize mechanical modeling involving finite element computational technologies to demonstrate that time-varying viscoelastic properties and growth are sufficient to account for the bulk of the FC morphogenetic changes.

© 2009 Published by Elsevier Inc.

Introduction

During development of multicellular organisms, morphogenetic movements of epithelial sheets generate organs of characteristic size and form. Cells within epithelial sheets cooperate to achieve a variety of distinctive shape changes. Invagination, evagination, folding, intercalation (convergent extension), cell flattening (epiboly), ingression, egression, and branching are widespread examples of epithelial morphogenesis (Fristrom, 1988; Pilot and Lecuit, 2005; Quintin et al., 2008). Cells within epithelia must coordinate adhesion, actin–myosin contractility, apical–basal and planar cell polarity during these movements. The analysis of how epithelial sheets accomplish morphogenesis is the first step to understanding and possibly preventing developmental and pathological abnormalities.

The growing field of epithelial morphogenesis requires model systems that are experimentally manipulable and accessible to imaging, and where these approaches can be integrated with measurement and modeling of mechanical forces. One such system is the *Drosophila* egg chamber. The egg chamber consists of a follicle cell (FC) epithelium that forms a coherent cell monolayer and encapsulates the growing germline, consisting of an oocyte along with its associated support or ‘nurse’

cells. Differential cell fate patterning in the early FCs prepares the epithelium to undergo a complex series of morphogenetic movements later in oogenesis. After cell division stops at stage 6 of ovarian development, the morphologically uniform FCs undergo four major and distinct morphogenetic events, described in the literature as posterior migration, squamous cell flattening, main body cell columnarization, and border cell migration (Deng and Bownes, 1998; Dobens and Raftery, 2000; Horne-Badovinac and Bilder, 2005; Spradling, 1993b; Wu et al., 2008). These events result in the characteristic organization and distribution of cells in the stage 10A egg chambers (Fig. 1A).

Posterior migration, squamous cell flattening and main body cell columnarization are initiated at stage 8 from the initially cuboidal FC epithelium, which is distributed homogeneously over the germline tissue. Posterior migration describes the striking reorganization of the egg chamber such that the vast majority of FCs come to overlie the posteriorly-positioned oocyte by stage 10A. These cells take on a distinctive, highly columnar morphology and eventually synthesize the eggshell; we will refer these hereafter as columnar-fated or columnar cells depending on their developmental stage. Concurrently, the most anterior FC in the cuboidal epithelium dramatically flatten to cover the nurse cells of the germline lineage; these cells, which we refer to as squamous-fated or squamous cells, have a minimal contribution to the final eggshell.

Over the last 16 years, migration of a subset of FCs called border cells has been intensively studied using molecular, genetic, imaging and other approaches (Bianco et al., 2007; Montell et al., 1992; Prasad and Montell, 2007; Rorth, 2002). The genetic and cellular requirements for border cell

* Corresponding authors. M.R.K. Mofrad is to be contacted at fax: +1 510 642 5835. D. Bilder, fax: +1 510 643 7448.

E-mail addresses: bilder@berkeley.edu (D. Bilder), mofrad@berkeley.edu (M.R.K. Mofrad).

¹ These authors contributed equally to the work.

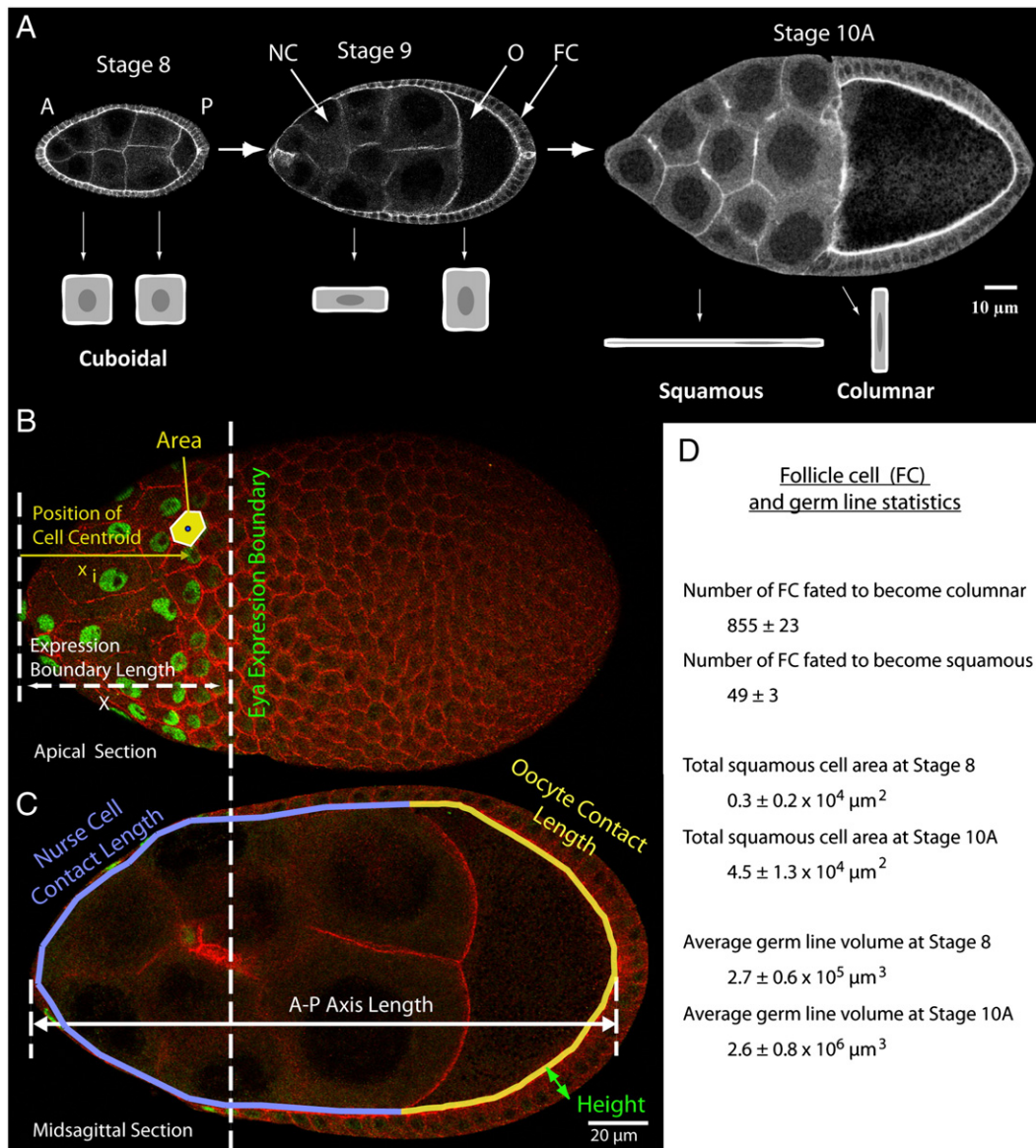


Fig. 1. Morphometric analysis of egg chambers. A: Midsagittal images of st. 8, 9, and 10A egg chambers stained for E-cadherin. The growth of the egg chamber, expansion of the oocyte (O) with respect to the nurse cells (NC), and diversification of the follicle cell (FC) epithelium into squamous and columnar populations can be seen. B, C: Illustration of parameters quantified on a stage 9 egg chamber stained for E-cadherin (red), and Eya (green) to mark squamous cells. FC positions, surface areas, height and length, as well as the contact surface area of germline and oocyte with these FCs are demarcated. D: Quantitation of FC numbers, areas, and cell volumes at stages 8 and 10A.

motility are increasingly well understood, and border cells have become a model for both normal multicellular motility and metastasis. In contrast, almost nothing is known about the mechanisms underlying posterior migration, which occurs at the same time and rate as border cell migration, nor about the alternate flattening and columnarization of the FC populations. Previous studies analyzing columnarization have proposed that it occurs due to an apical constriction mediated by the Beta-Heavy Spectrin-encoding gene *karst*, which is believed to shrink the apical surface and result in a complementary lengthening of the lateral cell domain (Zarnescu and Thomas, 1999). Additionally, apical contractility is thought to be a primary mechanism responsible for posterior migration by generating a ‘pulling force’ within the posterior-most FCs that draws columnar-fated FC towards and over the oocyte (Zarnescu and Thomas, 1999). Finally, this same force has been suggested to pull the squamous cells flat as the posterior columnarizing cells move away from the anterior pole (Grammont, 2007).

Studying the changes in cellular distributions and transitions between simple geometries—cuboidal, columnar and squamous—of the two FC populations provides an excellent opportunity to examine

fundamental morphogenetic processes in the same epithelial sheet. These changes occur in the absence of cell division, so the events can be attributed to mechanisms such as cellular mechanotransduction, migration and rearrangement, as well as, adhesion and cytoskeletal remodeling (Mofrad and Kamm, 2009). Here we have carried out an initial quantitative analysis, accompanied by mathematical modeling, of these familiar but little-studied morphogenetic events in order to establish the parameters of, shed light on and delimit the potential processes that regulate columnarization, cell flattening, and cell distribution within the FCs. Our results compel a striking revision of accepted views of these phenomena.

Materials and methods

Fly strains

All measurements were performed on *white* or *dpp-LacZ* (to identify squamous cells) flies. *Dicephalic* (*dic[1]*) mutants were obtained from the Bloomington Stock Center.

Immunohistochemistry

Egg chambers were fixed and stained as previously described (Horne-Badovinac and Bilder, 2008). Briefly, ovaries were dissected in phosphate buffered saline (PBS), fixed in 4% EM grade paraformaldehyde (Polysciences) in PBS. Primary antibodies were rabbit anti- β -galactosidase (1:2000, preabsorbed, Biogenesis), mouse anti-alpha-tubulin (Sigma, clone DM1A) and rat anti-E-Cadherin antibodies (Developmental Studies Hybridoma Bank). Fluorophore conjugated secondary antibodies were from Molecular Probes. Connective tissue and ovariole muscle sheath were mechanically removed by gentle micropipette resuspension.

Imaging and quantification

Confocal images of egg chambers were taken using a Leica TCS SL confocal microscope. FC apical surface images were quantified using scripts written for MATLAB Image Processing Toolbox (The Mathworks, Natick, MA). The apical surfaces of cells were outlined and the area was calculated along with a centroid. The centroid was used to identify the position of the cell along the A–P axis. To correlate the positions of columnar cells at different points during development, positions were normalized to the squamous/columnar cell boundary, as identified through expression of *dpp* (Dobens and Raftery, 2000; Twombly et al., 1996). Cell heights were quantified by measuring the length of the lateral cell membrane through a midsagittal plane image and again correlated to normalized positions from the *dpp* expression boundary. Volumes of individual cells along the *dpp* expression boundary were calculated using area and height data. Apical surface area of the entire egg chamber, the columnar FC epithelium or oocyte, and squamous cells or nurse cells was calculated through the midsagittal plane image of each chamber. Assuming an AP axisymmetric egg chamber, the apical surface area associated with the egg chamber is the surface created by a 360° rotation about the A–P axis of the apical surface. Analysis of individual columnar and future columnar cell dimensions were carried out on centrally located FCs due to geometric constraints (see legend to Fig. 3). Compliance was measured as the change in apical area of the entire squamous cell population divided by the change in FC-contacting surface area of the entire germline. Compliance of an equivalent number of columnar cells was calculated by assuming the total change in apical area of the follicle cell epithelium is equal to the total change in basal surface area of the entire germline. To count total follicle cell numbers, egg chambers were stained with Hoechst and nuclei were counted on cross-sectional images taken on Z16 APO microscope (Leica), fitted with a DFC300 FX camera. Further details about imaging and quantification processes can be found in (White, 2007).

Finite element analysis and modeling

All finite element models were generated in ADINA v8.3.1 (Automatic Dynamic Incremental Nonlinear Analysis, ADINA R&D Inc., Watertown, MA). ADINA is a software package for performing displacement and stress analysis using the finite element method. The FC epithelium was modeled using a temperature dependent viscoelastic material formulation with a Lagrangian formulation for large stresses and strains. This two parameter, viscoelastic Maxwell material model invoked a Williams–Landel–Ferry shift function (ADINA Theory and Modeling Guide, ADINA R&D Inc. Watertown, MA). Although significant thermal fluctuations do not generally occur during oogenesis in vivo, these thermal effects were used for the purpose of the finite element implementation. Thermal strain effects were used to model growth within the system, and strain was applied only to the basolateral domain to simulate columnarization.

The viscoelastic formulation is due to Holzapfel, a generalized Maxwell model with many chains comprised of springs of stiffness E and dashpots of viscosity η (Holzapfel, 1996). In our implementation,

only one chain was used, with previously established material constants for the baseline apical domain where $E=300$ Pa and $\eta=100$ Pa s (Karcher et al., 2003; Mofrad and Kamm, 2006). To simulate apical stiffness (Wang and Riechmann, 2007; Zarnescu and Thomas, 1999), we modeled the apical domains with elevated properties, with $\eta=2000$ Pa s. The material properties degrade to their baseline levels sequentially over time, starting at the anterior pole. The timing of the transition from elevated to baseline material properties was iterated until the simulated output matched morphometric data. The effect of the germline on the FCs is modeled as internal pressure. This pressure is exerted uniformly at a magnitude of 4.0×10^{-4} Pa. Given the material properties we implemented, this is sufficient to drive the deformations representing FC morphogenesis over the period of 6.25 h of simulated time, the estimated length of stage 9 (Spradling, 1993a). Altering the material property magnitudes would lead to a change in the required internal pressure and the timing of the material property transition. While the model would behave differently, this would not lead to changes in the conclusions of the model. The model is meshed with 1288 9-node 2-D axisymmetric elements. This assumes the egg chamber is axisymmetric along the A–P axis, an assumption that remains reasonable until stage 10 of oogenesis. The mesh is divided into 23 domains, the approximate number of FCs spanning from pole to pole along one arc (data not shown). Thus the material properties vary spatially in domains similar to the size of the cell. The apical domain has an initial thickness of 1 μm , and the basolateral domain had a thickness of 7 μm . The initial A–P axis length is 107 μm . Further details about the computational models and analyses can be found in (Shreter, 2007).

Results

Morphometric analysis of FC populations during mid-oogenesis

To systematically investigate the different types of epithelial reorganization that shape the egg chamber during oogenesis, we undertook a morphometric analysis, focusing particularly on follicle cell (FC) shape changes with respect to oocyte positioning between stages 8 and 10A. We used phalloidin, E-cadherin, or tubulin staining to demarcate the cortex of FCs, nurse cells, and oocytes, as well as nucleic acid-binding dyes to mark nuclei, and custom software to collate data obtained from confocal imaging (Figs. 1B, C). Until stage 8, the FC epithelium is uniformly cuboidal and measurements demonstrate that $29\% \pm 9\%$ (S.D., $n=8$) of FCs overlie the oocyte. During stage 9, the percentage of FCs over the oocyte increases to $56\% \pm 7\%$ (S.D., $n=18$); these take on an increasingly columnar FC morphology, while FCs that do not contact the oocyte flatten sequentially towards the anterior pole (Figs. 1A, D; 2C). The result is an anterior–posterior morphological gradient where FCs are more flat anteriorly and more columnar the closer they are positioned to the oocyte. At stage 10A, this transient morphological gradient has resolved into distinct columnar and squamous cell populations. The columnar-fated cells account for $95\% \pm 3\%$ (S.D., $n=10$) of the FCs and consist of cells fated to become centripetal migrating cells and so-called main body follicle cells (MBFC), which number 855 ± 23 (S.D., $n=13$). The dramatic shift in FC populations, from 29% to 95% of FC contacting the oocyte, has lent the term ‘posterior migration’ to this process, but the cellular events underlying it remain poorly understood.

During the time when the majority of FCs come into contact with the oocyte, 49 ± 3 (S.D., $n=8$), FCs at the anterior pole undergo dramatic flattening that leads to the formation of a squamous epithelium covering the nurse cells (Figs. 1A, D). During the process, the surface area occupied by squamous FCs increases 15-fold, from $0.3 \pm 0.2 \times 10^4 \mu\text{m}^2$ (S.D., $n=8$) to $4.5 \pm 1.3 \times 10^4 \mu\text{m}^2$ (S.D., $n=10$) (Fig. 2C). Flattening appears to occur sequentially, initiating in the most anterior FCs, and then propagating posteriorly to neighboring FCs (Grammont, 2007). This anterior to posterior sequential transition from cuboidal to

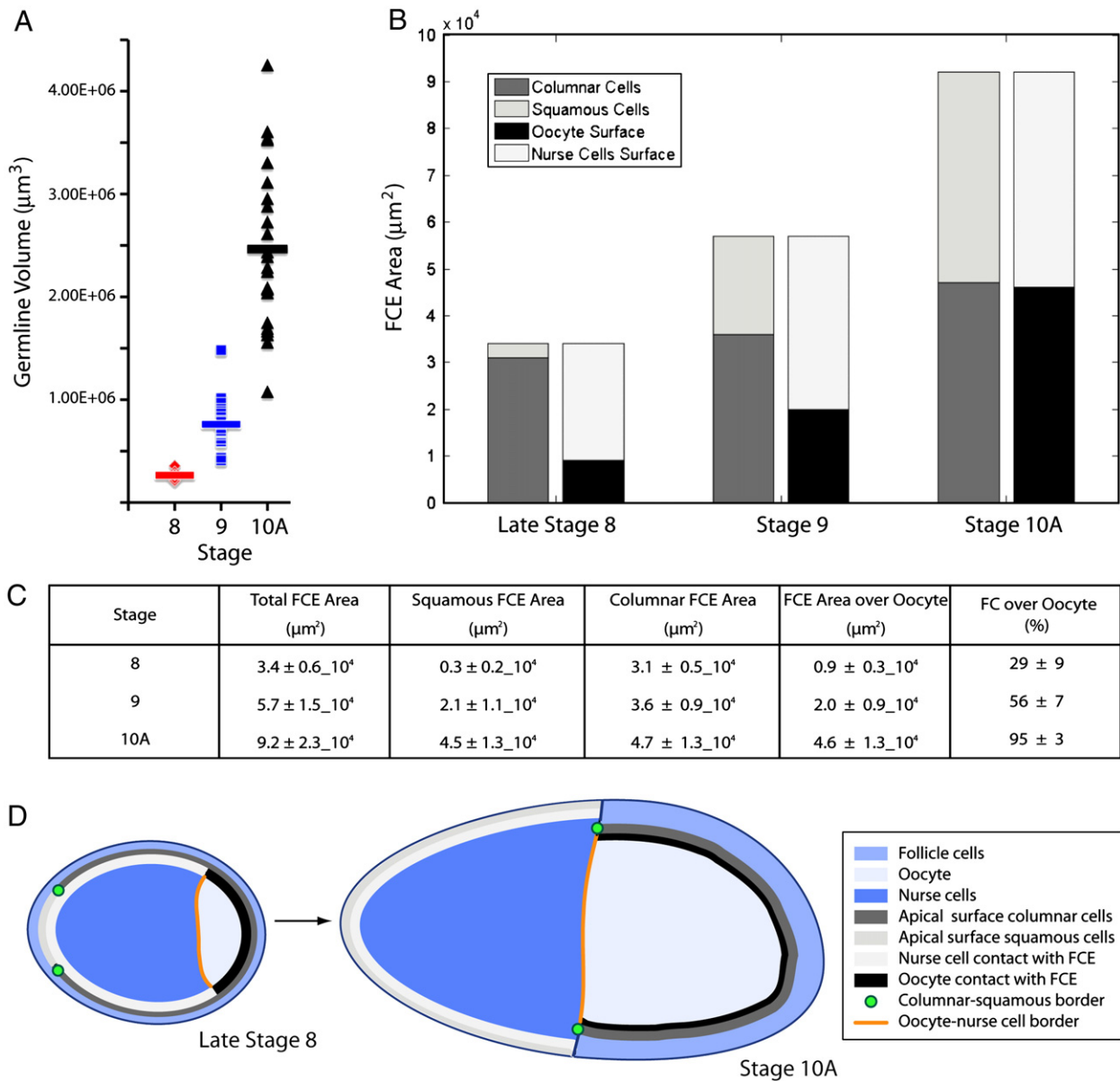


Fig. 2. Germline growth results in posterior displacement of FCs. **A:** Egg chamber volume plotted versus stage of oogenesis. Bars represent median values. The egg chambers undergo an ~10-fold increase in volume between stages 8 and 10A. **B:** Apportionment of follicle cell/germline (FC/GL) boundary area to individual FC and GL populations. For each stage, the left histogram presents the average total apical areas of the squamous and columnar FC populations, and the right histogram presents the average total apical areas of the oocyte and nurse cells. From stage 8 to 10A, the oocyte surface area (black) increases rapidly to take up a larger proportion of the FC/GL boundary, while the columnar FC surface area (grey) increases only slightly. **C:** Quantitation of FC areas and distributions at stages 8, 9 and 10A. **D:** Scaled diagram of stages 8 and 10A egg chambers, illustrating features associated with 'posterior migration'/'anterior accommodation'. While squamous FC apical surfaces areas as well as nurse cell and in particular oocyte volume all show extreme increases during these stages, the apical surface area of columnar cells (grey bar) changes much less drastically, resulting in redistribution of FCs over the oocyte.

squamous morphology occurs simultaneously with the columnarization in the posterior FC population. The biological machinery enabling these transitions is likely encoded by the differential cell fates established within the FC epithelium by developmental signaling pathways, such as JAK/STAT and EGF, prior to stage 8 (Horne-Badovinac and Bilder, 2005). However, the forces driving the parallel emergence of these different morphologies are little studied, yet provide an attractive system to study cell biological mechanisms in the context of environments governed by biomechanical principles.

'Posterior migration' of FCs occurs mainly by oocyte growth rather than FC movement

In order to evaluate current theories and to reveal unidentified mechanisms underlying these morphogenetic events, we quantified

selected morphological parameters of FCs and germline cells between stages 8 and 10A. We measured apical perimeter, volume, orientation and isometry of FCs. We also measured both surface area and volume changes in the oocyte and nurse cells. From stage 8 to stage 10A, the volume of the entire germline (oocyte + nurse cells) undergoes an average ten-fold increase from $2.7 \pm 0.6 \times 10^5 \mu\text{m}^3$ to $2.6 \pm 0.8 \times 10^6 \mu\text{m}^3$ (S.D., $n = 31$); this increase can be as much as 27-fold (Fig. 2A). The oocyte surface area that contacts FCs increases from $0.9 \pm 0.3 \times 10^4 \mu\text{m}^2$ to $4.6 \pm 1.3 \times 10^4 \mu\text{m}^2$ during posterior migration (Figs. 2B, C) (S.D., $n = 10$). This represents over a 500% increase in oocyte surface area. By comparison the nurse cells' surface area in contact with FCs increases only 80% during this period, from $2.5 \pm 0.4 \times 10^4 \mu\text{m}^2$ (S.D., $n = 8$) to $4.5 \pm 0.7 \times 10^4 \mu\text{m}^2$ (S.D., $n = 10$). Oocyte growth therefore accounts for 64% of total egg chamber surface area change, whereas nurse cell growth accounts

for 36% (Figs. 2B, C). Interestingly, this pronounced increase in oocyte volume and its associated increase in surface area results in a striking increase in area of oocyte–FC contacts.

The above measurements demonstrate that a rapid increase in oocyte surface directly causes the oocyte to come in contact with more FCs during stages 8 to 10A, when posterior migration is observed. In order to calculate the contribution that oocyte growth alone plays in posterior migration, we measured the oocyte surface area in contact with FCs and compared this to the columnar cell surface area during these stages. The results show that the combined apical surface area of all columnar FCs increases only 50%, from $3.1 \pm 0.5 \times 10^4 \mu\text{m}^2$ (S.D., $n = 8$) to $4.7 \pm 1.3 \times 10^4 \mu\text{m}^2$ (S.D., $n = 10$) (Figs. 2B, C); this is at the

same time that FC-contacting oocyte surface area increases by 500%. The rapid increase of oocyte surface area relative to that of columnar FCs reveals that oocyte growth towards the anterior, rather than migration of FCs to the posterior, leads to the observed arrangement of FCs at stage 10. ‘Posterior migration’, which implies active FC movement, is thus a misnomer; the perceived movement is an illusion caused by a relative change in the anterior oocyte boundary. We suggest instead the term ‘anterior accommodation’, to reflect the fact that it is the expansion of anterior, squamous FCs accommodating germline growth that results in the distinctive partitioning of FCs overlying oocyte and nurse cells at stage 10 (Fig. 2D).

FC columnarization involves lateral membrane growth and not primarily apical constriction

The columnar-fated FCs, which account for nearly 95% of the total FCs population, change shape from cuboidal to columnar as they contact the oocyte during stages 8–10A (Fig. 1A). Previous models proposed that this columnarization results from an apical constriction of columnar-fated FCs that reduces the total apical surface of the entire cell population and allows them to move over the oocyte (Grammont, 2007; Wu et al., 2008; Zarnescu and Thomas, 1999). However, as described above, our measurements indicate that total apical surface areas of future columnar FCs do not decrease during stages 8–10A, but in fact increase. Individually, the average apical surface area of an FC at the posterior pole increases from $23 \pm 4 \mu\text{m}^2$ (S.E., $n = 8$) at stage 8 to $35 \pm 5 \mu\text{m}^2$ (S.E., $n = 18$) at stage 9, and to $58 \pm 5 \mu\text{m}^2$ (S.E., $n = 10$) at stage 10A (Fig. 3A). Similarly, the apical surface area of an individual columnar-fated FC lying more anteriorly increases from $54 \pm 11 \mu\text{m}^2$ (S.E., $n = 8$) at stage 8 to $69 \pm 6 \mu\text{m}^2$ (S.E., $n = 18$) at stage 9, and $70 \pm 4 \mu\text{m}^2$ (S.E., $n = 10$) at stage 10A (Fig. 3A). These measurements reveal that columnar-fated FCs that eventually contact the oocyte do not decrease in apical surface area; therefore, their prominent columnarization must result from processes other than apical constriction.

Columnarization can occur if cell height increases proportionally faster than the apical surface area, concomitant with an overall increase in volume. We therefore measured the height increase of FCs to determine the relative growth of the apical and lateral surfaces during this period. The height of columnar FCs increases from $7.0 \pm 0.5 \mu\text{m}$ (S.E., $n = 8$) at stage 8 to $9.0 \pm 0.5 \mu\text{m}$ (S.E., $n = 18$) at stage 9, and to $13 \pm 0.7 \mu\text{m}$ (S.E., $n = 10$) at stage 10A (Fig. 3B). The ratio of apical surface area to height of anterior MBFCs is $7.8 \pm 0.7 \mu\text{m}$ (S.E., $n = 8$) at stage 8, $7.6 \pm 0.3 \mu\text{m}$ (S.E., $n = 18$) at stage 9, and $5.4 \pm 0.4 \mu\text{m}$ (S.E., $n = 10$) at stage 10A (Fig. 3B). Thus, the height of the columnar-fated FCs increases at a greater rate than the apical perimeter and results in the acquisition of columnar morphology despite their increasing apical surface area. Concomitantly, FC volumes increase as

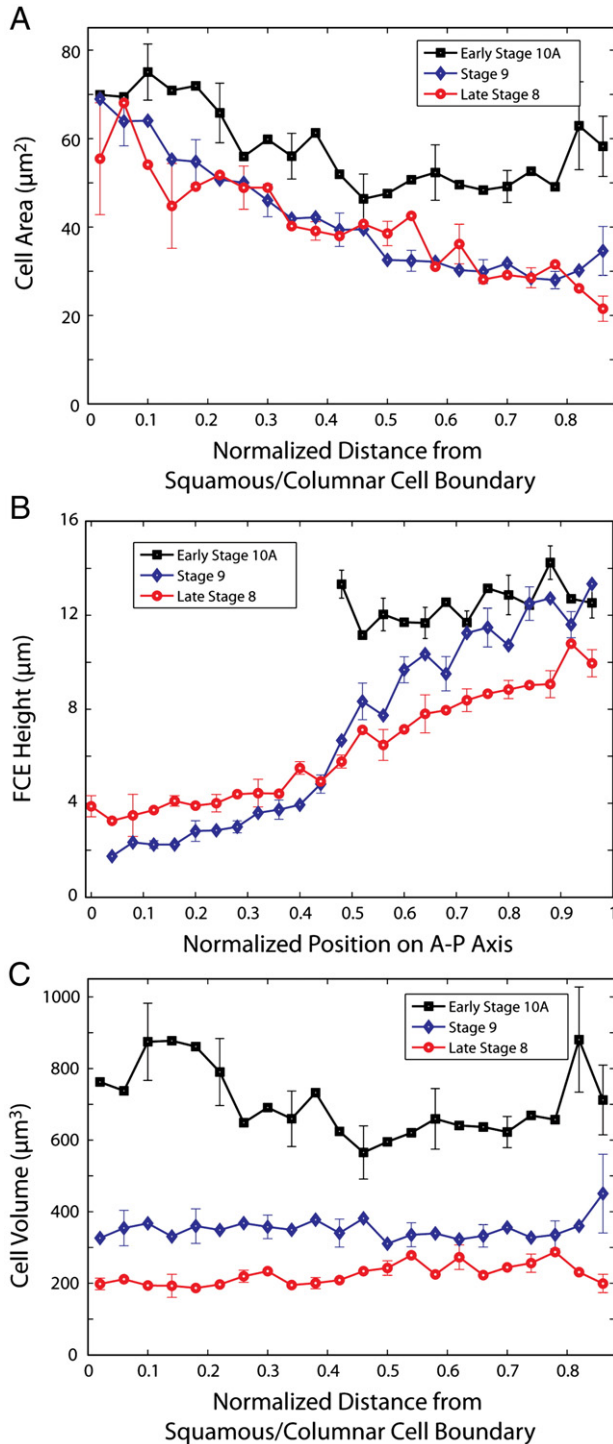


Fig. 3. Posterior FCs do not apically constrict during columnarization. **A:** Apical surface areas of single FCs as a function of normalized distance from the squamous/columnar cell boundary. Normalized distance is the position on the A–P axis relative to the Dpp expression boundary divided by the distance between the Dpp expression boundary and the posterior tip of the chamber; positive position indicates cells posterior to Dpp. Comparison at a given position reveals that apical surface areas of posterior cells increase rather than decrease during columnarization. Note that the measurements of most posterior cells may be affected by the geometry of projecting the curved surface of the egg chamber onto a two-dimensional image. Due to the steep curvature near the posterior pole, cell areas were only quantified on the anterior 90% of normalized distance from the columnar/squamous cell boundary, excluding the most curved posterior cells from the analysis. **B:** Heights of single FCs as a function of normalized position along the egg chamber A–P axis. Data for stages 8, 9 and 10A are shown; heights of anterior 10A are not shown since the extreme squamous morphology prevents accurate measurement. The trend at a given posterior position between stages reflects the progression of columnar morphology. In the anterior half of the egg chamber, FC heights decrease, reflecting the progression of squamous morphology. **C:** Volumes of FCs as a function of normalized distance from the squamous/columnar cell boundary. Cell volumes, which increase during oogenesis, are relatively consistent along the A–P axis. Volumes were calculated from apical perimeter and cell height measurements.

well (Fig. 2C). These data suggest that the expansion of the lateral membrane driven by cellular growth, rather than apical constriction, accounts for posterior FC columnarization.

Squamous FC morphology involves compliant stretching rather than active flattening

During stages 8–10A, the ~50 cuboidal FCs fated to become squamous flatten so extensively that their height at stage 10A is difficult to accurately measure (Figs. 1A, 2C). We explored the processes that might underlie this dramatic flattening. In a previous work, it was suggested that squamous cell morphogenesis involves active flattening generated by forces within the FCs (Grammont, 2007). The presumed reduction in surface area and migration of columnar FCs was proposed to flatten squamous-fated cells and draw them away from the anterior pole; alternatively, internally driven and outward-pushing flattening of squamous-fated cells could contribute to posterior displacement of columnar-fated cells. Based on our data above, we considered an alternative hypothesis: that a force generated by the rapidly growing germline results in tension that is responsible for the stretching of the squamous cells. In order to investigate these models, we calculated the compliance (see *Materials and methods*) of the two different FC populations, which reflects the proportion of germline growth that is accommodated by each population (Fig. 4A). If a given cell population flattens to accommodate all of germline growth, its compliance should equal 1. A compliance higher than 1 would reveal flattening faster than growth and point to an active FC cell-autonomous process. A compliance lower than 1 would indicate that that population was comparatively rigid; a negative compliance would indicate compression.

The compliance curve for all of the squamous cell population during stages 8–10A illustrates an interesting profile, in which three phases can be discerned (Fig. 4A). During stage 8, the compliance is 0.06, which is equivalent to the situation where all FCs are expanding their apical surfaces equally. However, during stage 9, the compliance of the squamous cells drastically shifts and closely approaches 1, indicating that flattening of the squamous FC population accommodates all of the germline growth during this stage (Fig. 4A). This perfectly-scaled response of squamous cells does not occur indefinitely; at the beginning of stage 10A the slope of the compliance curve strongly decreases to 0.25 (Fig. 4A). During this stage, the columnar cells also begin to contribute to the continuous expansion of the germline. Remarkably, these data demonstrate a precise regulation of flattening for these two FC populations during stages 8–10A. Moreover, during stage 9 the compliance measurements are consistent with an accommodating stretching response specifically of squamous cells to germline growth.

The observed flattening of squamous cells occurs during the time that the egg chamber is elongating in the anterior–posterior axis. To determine if squamous FC flatten isotropically or alternatively in a polarized fashion, we analyzed the aspect ratio between major and minor cell axis within the plane of the epithelium, which reflects anisometry of cell shape, and also measured the direction of this anisometry during stages 8–10A (Fig. 4B). Measurements show that squamous FCs increase their aspect ratio as flattening proceeds. At stage 8, 95% of the squamous FCs have an aspect ratio between 1 and 2, and the maximum aspect ratio measured is 2.3 (Fig. 4B). At stage 9, there are ~3 times (5% versus 14%) as many squamous FCs with aspect ratios greater than 2.0, and the maximum aspect ratio measured is 2.6 (Fig. 4B), revealing that squamous FCs do not flatten isotropically but instead are increasingly elongated. At stage 10, although the squamous FCs strongly decrease their flattening rate, their aspect ratios nevertheless increase even more dramatically: there are ten times (1% versus 10%) as many squamous FCs with aspect ratios greater than 2.5 at stage 10A as compared to stage 9, and the maximum aspect ratio measured is 3.6 (Fig. 4B). These data

demonstrate a strong trend of anisotropic squamous FCs elongation. We then calculated the direction of this elongation with respect to the anterior–posterior axis of the egg chamber. The data show that the major axis is on average oriented along the A–P axis, with the distribution of angles symmetric about this axis (Fig. 4C). Strikingly, out of the 353 squamous FCs measured, no cell demonstrates a major axis that deviates more than 50° from the egg chamber A–P axis. The flattening and elongation of squamous cells primarily along the A–P axis is consistent with compliant flattening in response to A–P egg chamber growth.

The data above suggest that growth of the oocyte and the germline is a major determinant of the morphology and arrangements of FCs in mid-oogenesis. To test this hypothesis, we extended our morphometric analysis to follicles mutant for *dicephalic* (*dic*). *Dic* egg chambers staged at 10A by morphological criteria (i.e. posterior oocyte covered by columnar FCs and anterior nurse cells covered by squamous FCs) exhibit less germline growth than WT egg chambers; our measurements show that germline growth is reduced by 46% and oocyte growth by 49% (Figs. 5A, B). Interestingly, average columnar FCE height and individual FC apical surface area are unchanged as compared to WT (Figs. 5A, C, D). In contrast, the average individual squamous FC apical surface area is reduced by 59% (Figs. 5A, C). Squamous FC numbers are increased and columnar FC numbers decreased in *dic* mutants (Fig. 5A), presumably because columnar-fated FCs unable to make contact with the undersized *dic* oocyte during stage 9 transition to a squamous fate. This phenomenon of columnar fate-plasticity has been previously reported for other mutants (Grammont, 2007) and may ensure that eggshell deposition by columnar FCs at later stages is limited to the oocyte surface. Nevertheless, the increase in *dic* squamous cell number is not sufficient to account for the decrease in individual cell area. In one example, a *dic* egg chamber with 107 squamous cells showed an average individual squamous cell surface area of 325 μm^2 . In a wild type egg chamber, a similar increase in squamous cell number would reduce the average surface area from 915 μm^2 to only 419 μm^2 . Thus, consistent with a decrease in *dic* germline volume, squamous cells appear to flatten even less than expected if normalized to cell number. Similar results were obtained using *egalitarian* and *mus301/spindleC* mutant egg chambers (data not shown). These data are consistent with three conclusions: first, even in mutants with reduced oocyte surface area, columnar-fated FCs do not migrate and constrict over the smaller oocyte. Instead, individual columnar FCs have area and height dimensions similar to WT suggesting fate-specific programming of cellular dimensions. Second, even in small germline mutant conditions, contact of columnar cells with the oocyte is determined by the extent of oocyte surface area increase. It is clear, however, that contact with the growing oocyte is required to maintain columnar fate and thus columnar surface area and height through stage 10A. Third, squamous cells appear to be extremely compliant to a wide range of germline volumes throughout stage 9; this drives their coordinated flattening towards the anterior until all nurse cells are equally accommodated by stage 10A.

An FEA model recapitulates key aspects of FC morphogenesis

Much of the biological data collected above are consistent with a central role for germline expansion in FC morphogenesis during stages 8–10A. Based on these data, we designed a simple computer model based on Finite Element Analysis (FEA) in order to explore the physical events at play. FEA is a frequently used mathematical approach that is capable of modeling biomechanical properties of multicellular systems with complex geometries and large ranges in stress/strain scales (Brodland and Clausi, 1994; Davidson et al., 1995; Holzapfel, 1996; Karcher et al., 2003). Our model considers internal pressure from a single expanding element (akin to a growing oocyte) imparting tensile forces onto many interconnected surrounding

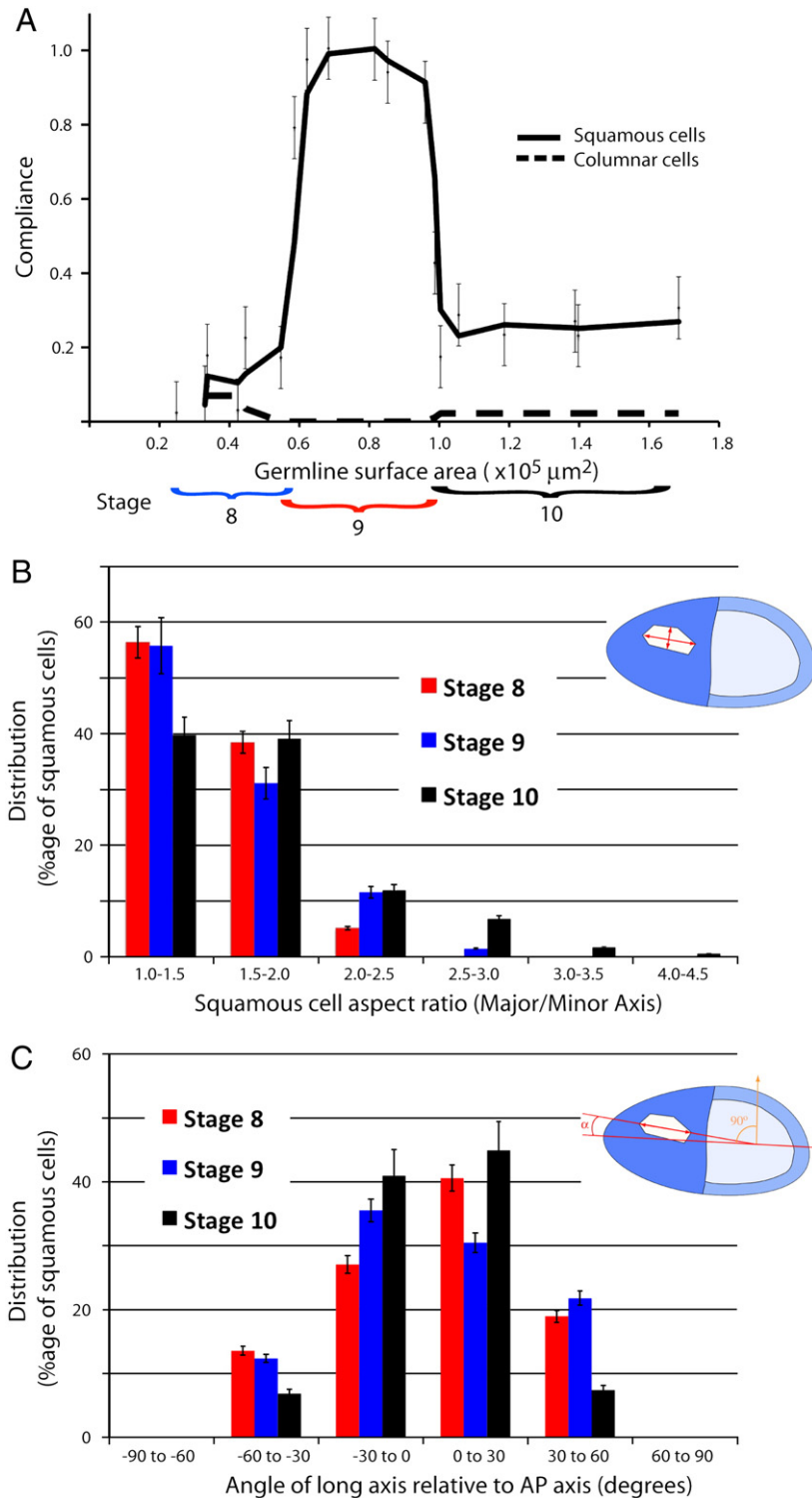


Fig. 4. Compliance and polarized flattening of anterior FCs transitioning to squamous morphology. **A:** The compliance of squamous and columnar FCs is plotted versus germline surface area, with stages of egg chamber development indicated below. Compliance (see text and *Materials and methods*) reflects the degree to which an individual FC population accommodates germline growth; the graph is normalized to squamous FC numbers. Note that at stage 8, squamous FC compliance is ~ 0.25 , indicating that all FCs stretch uniformly as growth occurs. At stage 9, compliance of squamous cells is 1, indicating that egg chamber growth is predominantly accommodated by squamous cell deformation. At stage 10A, squamous FC compliance returns to ~ 0.3 , indicating that the columnar FCs are now accommodating a significant proportion of egg chamber growth. **B:** Distribution of aspect ratios of squamous cells at different stages. Stage 10A egg chambers have more highly elongated and fewer unelongated anterior FCs than stage 8. **C:** Polarization of squamous cell elongation. The angle of the major axis relative to A–P axis illustrates that the squamous FCs elongate preferentially along the A–P axis at all stages.

elements (akin to the FC epithelial layer) (Figs. 6A, B). The dimensions of oocyte and FCs and time scale of the model roughly correspond to that established for stage 9. As our measurements revealed that FC volumes increased consistently through these stages (Fig. 3A), we incorporated this feature into the model. We varied cellular viscosities

rather than cellular stiffness or elastic modulus since the latter would imply that the cell shape changes observed would be instantaneously reversible; additionally, over the given timescale viscous forces should dominate. We modeled FC adhesion by allowing a transmission of stresses through the FC-like domains. Finally, to employ temporally

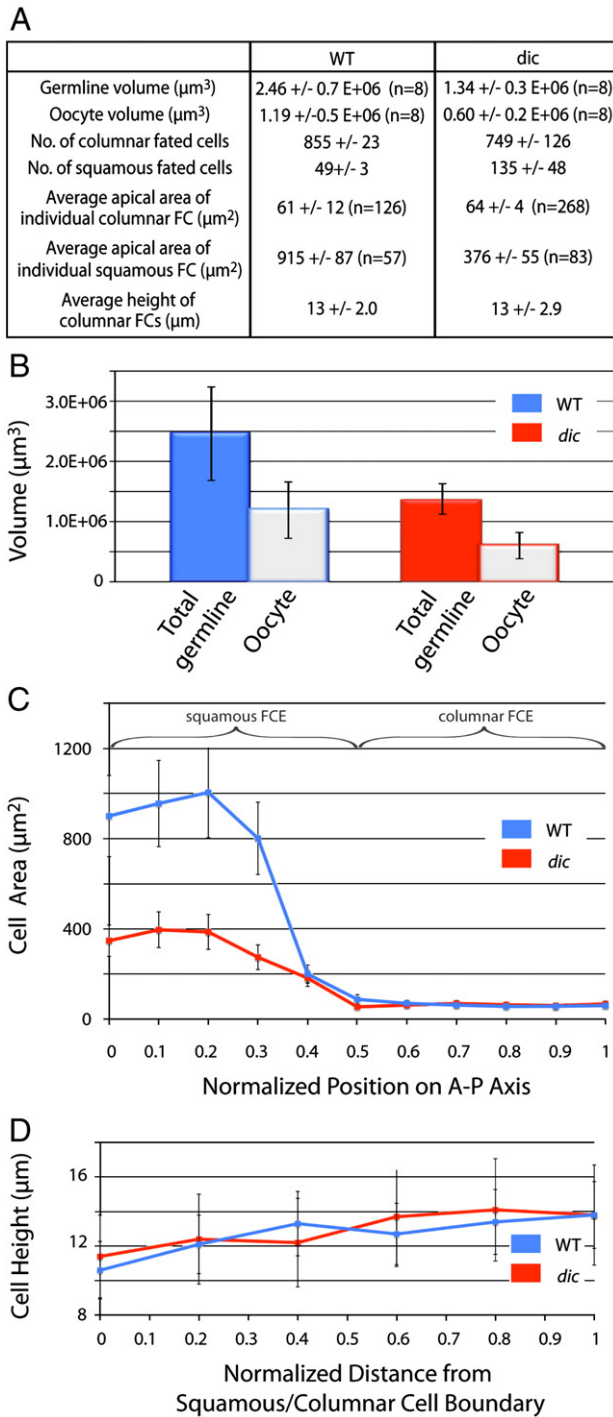


Fig. 5. Morphometric analysis of small germline mutant egg chambers. **A:** Quantitation of FC numbers, areas, and germline volumes in WT and *dicephalic* (*dic*) mutant follicles at stage 10A. **B:** Germline and oocyte volumes in WT (blue) and *dic* (red) mutants at stage 10A ($n = 8$, SD shown). **C:** Apical surface areas of single FCs in WT (blue) and *dic* (red) at stage 10A as a function of normalized distance along the egg chamber A–P axis. Columnar FCs have the same apical area in both genotypes; however, squamous cells are much smaller in *dic* follicles. **D:** Heights of single FCs in WT (blue) and *dic* (red) as a function of normalized position along the egg chamber A–P axis at stage 10A. By extension, cell volumes of columnar FCs in WT and *dic* follicles are similar.

and spatially changing properties in FC adhesion, we implemented a material breakdown in our FEA similar to the sequentially posterior propagating adherens junction breakdown observed in stage 9 egg chambers (Grammont, 2007).

Execution of the model reveals that FCs with intact intracellular adhesion do not deform greatly as the oocyte expands, while FCs in

which intracellular adhesion breaks down flatten to rapidly become squamous (Figs. 6C, D). To result in the accurate height profile (Fig. 6E) and timing of FC epithelial morphogenesis during stages 8–10A, the timing of this breakdown was iteratively deduced to follow a logarithmic-like curve. The curve contains a point of inflection, which does not correspond to a known anatomical landmark within the egg chamber, and occurs within the population of squamous cells (Fig. 6F). If the timing of this viscosity shift were varied from that in Fig. 5F, the cells would flatten either too quickly or too slowly. Additionally, a viscosity shift in the columnar-fated cells was required to account for their increase in apical dimensions. Columnarization of posterior FCs required the consistent increase in volume indicated by our measurements (Fig. 3C). The initial dimensions in the model, which represent a uniform cuboidal FC population with a height of 8 μm , evolve to describe anterior squamous FCs of 2 μm height and posterior columnar FCs with 14 μm height; these closely approximate our measurements for stage 9 FCs (Fig. 6E). No modeling of active FC movement nor of apical constriction was included and these were not required to recapitulate the FC morphological gradient between the anterior squamous FCs and the posterior columnar FCs. In sum, a mechanical model including only these simple elements—germline and FCE growth and differential material properties of the FCE—is sufficient to result in features of FC morphogenesis seen during ‘posterior migration’/anterior accommodation.

Discussion

Redefining poster migration as anterior accommodation

45 years ago, Koch and King (Koch, 1963) suggested that columnar-fated FCs come to lie over the oocyte at stage 10 via active movement of FCs towards the posterior pole. Since that time, this process has been described as posterior migration (Deng and Bownes, 1998; Dobens and Raftery, 2000; Horne-Badovinac and Bilder, 2005; Spradling, 1993b; Wu et al., 2008). The fact that posterior migration occurs during the same developmental stages and with a similar speed to the well-characterized border cell migration—indeed, border cell migration is often benchmarked by posterior migration—lent credence to the notion of active FC motility. However, in contrast to border cell migration, the genetic, molecular, and developmental events that lead to this striking cellular distribution have remained unknown.

Our quantitative morphometric analysis of FC morphogenesis between stages 8 and 10A reveals that the apparent migration of columnar-fated FC over the oocyte is in fact an illusion. The data show that total apical surface area of the (cuboidal) columnar-fated FCs in a stage 8 egg chamber is smaller than the total apical surface areas of the columnar FCs at stage 10A. However, as the oocyte increases ten-fold in volume during these stages, its growing surface area contacts threefold more overlying FCs (from 29% to 95%) as it displaces the nurse cells anteriorly. Nurse cell displacement is then accommodated by the flattening and dramatic increase in surface area of squamous-fated cells. One outstanding issue is the mechanisms that constrain germline growth in the A–P axis, which is a fascinating area of study not addressed here (Bateman et al., 2001; Frydman and Spradling, 2001).

We conclude that there is no net movement of columnar-fated FCs along the A–P axis during these stages, and that growth of the oocyte underneath the columnar FC in wild type and small germline mutant egg chambers is sufficient to account for the final distribution of FCs. We therefore propose an alternative term for posterior migration: anterior accommodation. This term reflects the non-motile role of posterior columnar cells and the dynamic reshaping of anterior squamous-fated cells that accommodate the growing germline and anteriorly expanding oocyte (Fig. 2C). The absence of an active migratory activity in FCs is consistent with the failure of FC mosaic screens to isolate mutations that affect the process (unpublished results, see Kolahi, 2009) and serves to

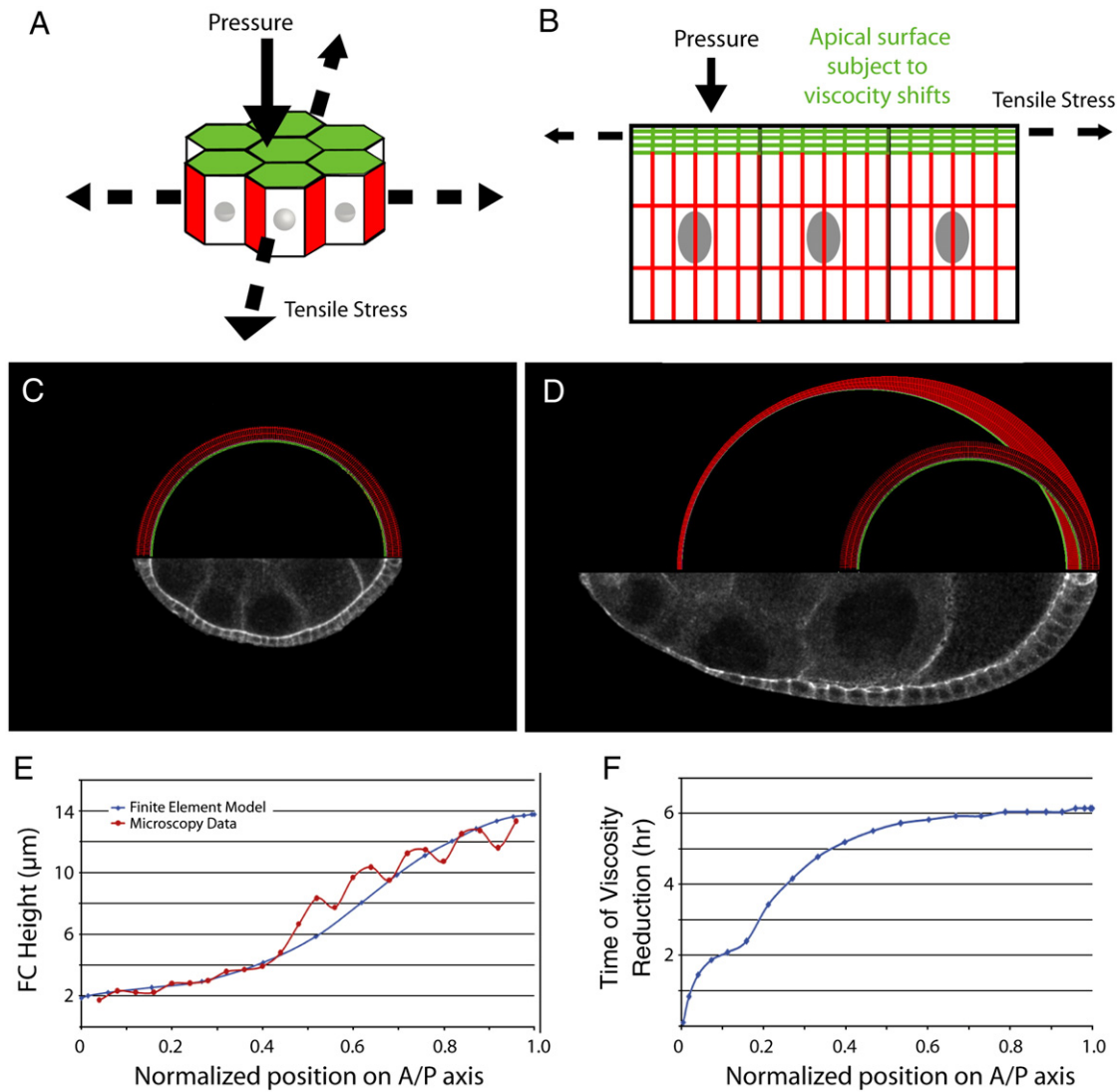


Fig. 6. Mechanical modeling of FC heights. A: Schematic illustrating parameters of FC epithelia modeled in FEA. FCs grow through biosynthesis and are subject to a uniform pressure from the growing germline imparting isotropic tensile stress onto their apical surface. B: Several FEA elements represent the body of a cell (red). The FEA elements representing the apical domain (green) are subjected to viscosity shifts in the model. All elements grow as modeled by thermal expansion to reflect cellular growth during stage 8–10A (see [Materials and methods](#)). C: Initial state of the model (above) in comparison to a stage 8 egg chamber (below). The uniform heights in the initial mesh match parameters of the egg chamber. D: Initial (crosshatched) and deformed (solid) meshes at model completion, in comparison to the gradient of FC morphologies in a stage 9 egg chamber (below). As the cells on the right remain stiffer, they grow more preferentially along their lateral domains to become more columnar, and resist flattening more than cells on the left that become squamous. Note that overall elongation of the egg chamber along the A–P axis is not captured by the set of parameters modeled. E: Comparison of final FC heights, as a function of A/P axis position, displayed in the egg chamber (red) with those produced by the FEA model. F: Timing of viscosity reduction within the FEA model as a function of A/P axis position. These parameters are required to generate the solution shown in C and D. See text for discussion.

redirect investigations of FC morphogenesis towards the role of germline growth and its associated forces.

Columnarization of posterior follicle cells is driven by cellular growth

Apical constriction mediated by the actomyosin cytoskeleton is a widespread mode of epithelial morphogenesis, best studied in metazoan gastrulation and neurulation (Pilot and Lecuit, 2005). Cells subject to apical constriction can dramatically change shape and elongate, as exemplified by invaginating bottle cells of *Xenopus* (Lee and Harland, 2007). Such examples made plausible previous models proposing that apical constriction of columnar FCs could account for their apparent elongation in the apical–basal axis. However, our data indicates that columnar-fated cells do not contract their apical perimeter during columnarization, but actually slightly increase it. We find that columnarization instead results because the increased volume of the FCs is largely channeled into growth of lateral

membrane domains, which is threefold greater than that of the apical membrane. There are at least three possibilities how FCs could accomplish such nearly unidimensional growth: direct biosynthetic delivery exclusively to the lateral membrane, relatively isometric delivery to all cell surfaces matched by increased apical endocytosis, or isometric delivery accompanied by a continuous apical migration of the zonula adherens. Our current data do not allow us to distinguish between these possibilities. In addition to pointing to modes of columnarization, the absence of an apical constriction has important implications for the mechanisms underlying FC distributions. Previous models have proposed that apical constriction during columnarization results in a ‘pulling force’ that contributes to migration of FCs over the oocyte (Zarnescu and Thomas, 1999). Our results pointing to oocyte growth rather than FC motility driving anterior expansion mean that a ‘pulling force’ does not have to be invoked.

Our observation that the apical surface of columnar-fated FCs increases between stages 8 and 10A was unexpected. From a

biomechanical perspective, this increase in apical area could result from pressure exerted by the growing germline on columnar FCs. There is evidence that FCs resist this tensile stress by apically localizing cytoskeletal specializations. The Beta-heavy Spectrin molecule *Karst* is required to assemble a stable spectrin skeleton at the apical surface of FC; *Karst* mutant FCs have enlarged apical surface areas, suggesting that a submembrane spectrin-based contractility is required to maintain apical cell perimeter (Zarnescu and Thomas, 1999). Additionally, actomyosin activity in early FCs specifically localizes to the apical domain, and disruption of this activity results in expansion of apical FC surfaces and flattening in response to pressure from the growing germline (Wang and Riechmann, 2007). This localized actomyosin activity may correspond to the actin-linked spectrin-cytoskeleton maintained by *Karst*. The resemblance of flattening seen in loss of apical actomyosin contractility to normal squamous development is striking and may point to a possible mechanism of squamous cell morphogenesis in addition to the adherens junction breakdown documented by Grammont (2007).

Compliance to germline growth may underlie squamous cell flattening

The developmentally regulated flattening of squamous FCs in the anterior of the egg chamber is strikingly converse to the columnarization of posterior FCs. Like columnarization, squamous transitions are widespread in epithelial morphogenesis, but the modes that underlie them are only beginning to be explored. It appears that flattening arises from a force experienced by the anterior FCs, but three distinct origins for such a force can be envisaged. First, as previously proposed (Grammont, 2007; Zarnescu and Thomas, 1999), an absolute migratory movement of columnarizing FCs could generate a posteriorly-directed 'pulling force' in the plane of the epithelium that stretches the anterior FCs. Second, active and cell-autonomous processes within each anterior FC that rearrange their cytoskeletons could exert internal forces that drive flattening and elongation of the anterior–posterior axis. Third, the major force could originate not in the plane of the FC epithelium but in a plane perpendicular: a 'pushing' force arising from germline growth that compresses the FCs in the apicobasal axis, and leads to their flattening and elongation along the A–P axis as a consequence.

Our calculation of the compliance of the FCs provides a starting point for consideration of the above three models. By comparing the compliance of the squamous-fated FCs versus the columnar-fated FCs, one can infer whether internal or external forces may drive flattening of squamous-fated cells. Compliance is defined in mechanical sciences as the ability of an object to yield elastically when a force is applied. The compliance curve measures how increases in FC surface area relate to interior germline expansion. Since the FC epithelium is contiguous and intimately associated with the interior germline, the germline surface area and total FC apical surface areas are equivalent; thus, the compliance of the entire FC epithelium is 1. The compliance of the two FC populations at stage 8 is equal, reflecting the fact that at this stage both populations respond to germline growth identically. At stage 9, however, compliance of the populations diverges. In the first two models mentioned above, a pulling force from true posterior migration or cell-autonomously driven flattening would generate a negative compliance in the columnar-fated FCs, and an increase in compliance of squamous-fated FCs beyond 1. This would reflect how squamous cells would try to accommodate the surface deficit resulting from the migration in model 1, or how in model 2, intrinsically flattening cells may push outwards and compress posterior cells. However, the data indicate that squamous FC compliance never exceeds 1 and columnar FC compliance is never negative. We propose that this reflects the absence of true migration of posterior FCs along the germline boundary and indicates that squamous cells do not proportionally flatten faster than the germline area increases, as might be expected if cells flatten actively and independently of germline growth.

Instead, during stage 9, the compliance of the squamous-fated cells closely approaches but does not exceed 1, while the compliance of the columnar-fated FCs closely approaches 0. A compliance of 1 is what would be expected if the third case—flattening of the squamous cells in response to and dependent on germline pressure—was occurring. We note that the relative stiffness of columnar FCs with a compliance of nearly 0 may provide an anchoring point for squamous-fated cells from which their flattening is driven towards the anterior. This is supported by the observation that columnar cells in small germline mutant egg chambers have apical surface areas and height dimensions similar to WT cells, whereas squamous cells have reduced apical areas indicating that the extent of flattening varies proportionally to germline volume increase. Notably, this accommodative flattening is regulated: during stage 10A, compliance of the columnar FCs returns while that of the squamous FCs decreases. This response suggests that the columnar FCs decrease their resistance to flattening. It is intriguing to speculate that this shift in compliance may allow columnar FC to sense and precisely accommodate oocyte growth to ensure perfect coverage of the oocyte surface for eggshell deposition.

Recently, an interesting mechanism for squamous transitions in the embryonic amnioserosa has been described, involving wholesale rotation and elongation of the microtubule cytoskeleton within transitioning cells (Pope and Harris, 2008). Such a mechanism, in line with the second proposed above, is not ruled out by our data. However, we note that the amnioseroal flattening occurs in a tissue of constant volume where no expansionary forces are experienced, and that adherens junctions remain intact throughout the process, while in the FC epithelium squamous cell flattening is associated with disassembly or loss of adherens junctions.

We therefore favor a model where FC squamous cell transition results primarily as a response to germline growth, without involving forces generated within FCs. Formally, the germline increase in volume must exert a pressure on the overlying FCs, and indeed data reveal that this force must be actively resisted by FCs to maintain their morphology after stage 5. The resistance to counterbalance the tensile forces imparted by germline expansion requires apical myosin activity in FCs (Wang and Riechmann, 2007). We suggest that alterations in this activity, as a result of or perhaps driving adherens junction disassembly, lead to compliant flattening of anterior FCs in response to germline growth, eventually resulting in the cubodial to squamous transition. Explicit measurements of the germline tension that is generated will be of considerable importance to future studies of egg chamber morphogenesis.

Using FEA to model follicle cell morphogenesis

We created an FEA computational model of FC morphogenesis to test whether germline and follicle cell growth, as well as regulation of FC apical stiffness could account for the characteristic FC morphology observed at stage 10A. The computational model takes into account the biomechanical events that must occur during FC shape transitions. Our morphometric data do not support any active migration of columnar-fated FCs to the posterior pole, and thus no FC movement was modeled.

In the FEA model, we simulated a constant expansionary growth of the germline and FC size. In vivo and in the model, the increase in germline and FC volume will create a pressure that exerts tensile stresses on the apical domain of an integral FC epithelium confined within a sheet. We approximated the magnitude of this tensile stress through the material property assumptions of the epithelium (see *Materials and methods*). Given that apical contractility is required to prevent FC flattening (Wang and Riechmann, 2007), we wondered whether modulation of apical stiffness could account for flattening of anterior cells. We thus implemented a material breakdown by decreasing viscosity of the apical domain in an anterior–posterior propagated manner based on observations by Grammont (2007). The

timing of this propagation had to be modified iteratively, but using it we could accurately recapitulate the given height data and duration of FC morphogenesis. Interestingly, in the model, eliminating pressure from a germline growth caused anterior cells to remain cuboidal whereas posterior cells still columnarized (data not shown, see Shreter, 2007). Nevertheless, a key requirement to recapitulate posterior columnarization was the implementation of a consistent volume increase within FC analogous to the growth we observed during our morphometric analysis of egg chambers during the stages 8–10A.

Our model points to the key relationship between germline growth and FC material properties. In the model, we tested how FC morphogenesis can result from changes in apical face integrity in the presence of growing germline pressure. Modeling indicates that a gradient in the material properties, or cell stiffness, along the A–P axis is sufficient to cause the characteristic cell shape gradient. Temporal and spatial regulated breakdown of the adherens junctions of FCs could generate the stiffness gradient, although we note that we modeled apical domain stiffness, mirroring evidence for a myosin and spectrin-based web that underlies apical face integrity rather than junctional contractility (Wang and Riechmann, 2007; Zarnescu and Thomas, 1999).

The morphometric data obtained and implemented into the model simply describe the end points of cell shape transitions, and the path taken to these end points may vary from that in the model. Nevertheless, our FEA model captures the spatiotemporal dimensions of FC shape transitions for a reasonable set of parameters. The models do not explicitly test every factor involved in FC morphogenesis; however, they do explore what net physical changes must take place. Representing a more precise cytoskeletal organization by including anisotropic cell properties can further refine the model. In future iterations of FC modeling, orthotropic material properties could likely capture additional detailed features of egg chamber morphogenesis, such as the mechanisms that restrict growth along the dorsoventral perimeter and those that result in the pointed anterior tip.

Acknowledgments

MRKM thanks Dr. Stas Shvartsman for introducing him to *Drosophila* oogenesis. PFW and DMS also gratefully appreciate insightful conversations with Dr. Shvartsman at the initial phase of this work. We thank the Bloomington Stock Center and the Developmental Studies Hybridoma Bank for providing reagents. The authors are thankful to members of both the Bilder and Mofrad labs for their invaluable input. This work was supported by the UC Berkeley start-up funds, Regents' Junior Faculty Fellowship, and a grant by the National Science Foundation (CBET0829205) to MRKM and by grants from the NIH (R01 GM068675) and the Burroughs Wellcome Trust to D.B. PFW was supported by a National Science Foundation Graduate Student Fellowship, KSK was supported in part by a National Institutes of Health NRSA Training Grant (NIH 5 T32 HG00047), and A-K.C was supported by a fellowship from the Jane Coffin Childs Memorial Foundation.

References

Bateman, J., Reddy, R.S., Saito, H., Van Vactor, D., 2001. The receptor tyrosine phosphatase Dlar and integrins organize actin filaments in the *Drosophila* follicular epithelium. *Curr. Biol.* 11, 1317–1327.

Bianco, A., Poukkala, M., Cliffe, A., Mathieu, J., Luque, C.M., Fulga, T.A., Rorth, P., 2007. Two distinct modes of guidance signalling during collective migration of border cells. *Nature* 448, 362–365.

Brodland, G.W., Clausi, D.A., 1994. Embryonic tissue morphogenesis modeled by FEM. *J. Biomech. Eng.* 116, 146–155.

Davidson, L.A., Koehl, M.A., Keller, R., Oster, G.F., 1995. How do sea urchins invaginate? Using biomechanics to distinguish between mechanisms of primary invagination. *Development* 121, 2005–2018.

Deng, W.M., Bownes, M., 1998. Patterning and morphogenesis of the follicle cell epithelium during *Drosophila* oogenesis. *Int. J. Dev. Biol.* 42, 541–552.

Dobens, L.L., Raftery, L.A., 2000. Integration of epithelial patterning and morphogenesis in *Drosophila* ovarian follicle cells. *Dev. Dyn.* 218, 80–93.

Fristrom, D., 1988. The cellular basis of epithelial morphogenesis. A review. *Tissue Cell* 20, 645–690.

Frydman, H.M., Spradling, A.C., 2001. The receptor-like tyrosine phosphatase lar is required for epithelial planar polarity and for axis determination within *Drosophila* ovarian follicles. *Development* 128, 3209–3220.

Grammont, M., 2007. Adherens junction remodeling by the Notch pathway in *Drosophila melanogaster* oogenesis. *J. Cell Biol.* 177, 139–150.

Holzappel, G., 1996. On large strain viscoelasticity: continuum formulation and finite element applications to elastomeric structures. *Int. J. Numer. Methods Eng.* 39, 3903–3926.

Horne-Badovinac, S., Bilder, D., 2005. Mass transit: epithelial morphogenesis in the *Drosophila* egg chamber. *Dev. Dyn.* 232, 559–574.

Horne-Badovinac, S., Bilder, D., 2008. Dynein regulates epithelial polarity and the apical localization of Stardust A mRNA. *PLoS Genet.* 4, e8.

Karcher, H., Lammerding, J., Huang, H., Lee, R.T., Kamm, R.D., Kaazempur-Mofrad, M.R., 2003. A three-dimensional viscoelastic model for cell deformation with experimental verification. *Biophys. J.* 85, 3336–3349.

Koch, R.K.A.E., 1963. Studies on the ovarian follicle cells of *Drosophila*. *Q. J. Microsc. Sci.* 104, 297–320.

Kolahi, K.S., 2009. Intertissue Mechanotransduction: Molecular Cell Biomechanics of Morphogenesis in *Drosophila melanogaster* Oogenesis. Master of Science Thesis. Molecular Cell Biomechanics Laboratory, Department of Bioengineering, The University of California Berkeley, CA, USA.

Lee, J.Y., Harland, R.M., 2007. Actomyosin contractility and microtubules drive apical constriction in *Xenopus* bottle cells. *Dev. Biol.* 311, 40–52.

Mofrad, M.R.K., Kamm, R.D., 2006. *Cytoskeletal Mechanics: Models and Measurements*. Cambridge University Press, New York, NY.

Mofrad, M.R.K., Kamm, R.D., 2009. *Cellular Mechanotransduction: Diverse Perspectives from Molecules to Tissue*. Cambridge University Press, New York, NY.

Montell, D.J., Rorth, P., Spradling, A.C., 1992. Slow border cells, a locus required for a developmentally regulated cell migration during oogenesis, encodes *Drosophila C/EBP*. *Cell* 71, 51–62.

Pilot, F., Lecuit, T., 2005. Compartmentalized morphogenesis in epithelia: from cell to tissue shape. *Dev. Dyn.* 232, 685–694.

Pope, K.L., Harris, T.J., 2008. Control of cell flattening and junctional remodeling during squamous epithelial morphogenesis in *Drosophila*. *Development* 135, 2227–2238.

Prasad, M., Montell, D.J., 2007. Cellular and molecular mechanisms of border cell migration analyzed using time-lapse live-cell imaging. *Dev. Cell* 12, 997–1005.

Quintin, S., Gally, C., Labouesse, M., 2008. Epithelial morphogenesis in embryos: asymmetries, motors and brakes. *Trends Genet.* 24, 221–230.

Rorth, P., 2002. Initiating and guiding migration: lessons from border cells. *Trends Cell Biol.* 12, 325–331.

Shreter, D., 2007. Computational Modeling of Epithelial Mechanics in *Drosophila melanogaster* Oogenesis. Master of Science Thesis. Molecular Cell Biomechanics Laboratory, Department of Bioengineering, The University of California Berkeley, CA, USA.

Spradling, A.C., 1993a. Developmental genetics of oogenesis. In: Arias, M. (Ed.), *The Development of Drosophila Melanogaster*. New York, Cold Spring Harbor Laboratory Press, pp. 1–70.

Spradling, A.C., 1993b. Germline cysts: communes that work. *Cell* 72, 649–651.

Twombly, V., Blackman, R.K., Jin, H., Graff, J.M., Padgett, R.W., Gelbart, W.M., 1996. The TGF-beta signaling pathway is essential for *Drosophila* oogenesis. *Development* 122, 1555–1565.

Wang, Y., Riechmann, V., 2007. The role of the actomyosin cytoskeleton in coordination of tissue growth during *Drosophila* oogenesis. *Curr. Biol.* 17, 1349–1355.

White, P.F., 2007. Mechanics of Epithelial Morphogenesis in *Drosophila melanogaster* Oogenesis: New Insights Based on Quantitative Morphometric Analysis and Mechanical Modeling. Master of Science Thesis. Molecular Cell Biomechanics Laboratory, Department of Mechanical Engineering, The University of California, Berkeley, CA, USA.

Wu, X., Tanwar, P.S., Raftery, L.A., 2008. *Drosophila* follicle cells: morphogenesis in an eggshell. *Semin. Cell Dev. Biol.* 19, 271–282.

Zarnescu, D.C., Thomas, G.H., 1999. Apical spectrin is essential for epithelial morphogenesis but not apicobasal polarity in *Drosophila*. *J. Cell Biol.* 146, 1075–1086.